applied sciences

MDPI

Article

Integrating the Finite Element Method with Python Scripting to Assess Mining Impacts on Surface Deformations

Mateusz Dudek [1], Dawid Mrocheń [1,*], Anton Sroka [1] and Krzysztof Tajduś [2]

[1] Division of Rock Deformation, Strata Mechanics Research Institute, Polish Academy of Science, 30059 Krakow, Poland; dudek@imgpan.pl (M.D.); sroka@imgpan.pl (A.S.)
[2] Faculty of Drilling, Oil and Gas, AGH University of Krakow, 30059 Krakow, Poland; ktajdus@agh.edu.pl
* Correspondence: dawid.mrochen@imgpan.pl

Abstract: Mining operations disrupt the structure of rock layers, leading to surface deformations and potential mining damage. This issue has been extensively studied since the 19th century using various analytical, geometric-integral, and stochastic methods. Since the 1990s, numerical methods have been increasingly applied to determine changes in the stress and strain states of rock masses due to mining activities. These methods account for numerous additional factors influencing surface deformation, offering significant advantages over classical approaches. However, modelling rock masses presents challenges, particularly in calibrating the mechanical parameters of rock layers, an area extensively researched with numerous publications. In this study, we determined the mechanical parameter values of rock layers at the advancing mining front using a custom Python script and Finite Element Method (FEM) numerical models. We also introduced a modification to evaluate the error of the estimated parameter values. Numerical analyses were conducted for the Piast–Ziemowit mine region in Poland, utilizing mining, geological, and surveying data. Our results demonstrate that accurate calibration of mechanical parameters is crucial for reliable predictions of surface deformations. The proposed methodology enhances the precision of numerical models, providing a more robust framework for assessing the impact of mining activities on rock layers.

Keywords: FEM; coal mining; surface deformation; strong layer; Python

Citation: Dudek, M.; Mrocheń, D.; Sroka, A.; Tajduś, K. Integrating the Finite Element Method with Python Scripting to Assess Mining Impacts on Surface Deformations. *Appl. Sci.* **2024**, *14*, 7797. https://doi.org/10.3390/app14177797

Academic Editors: Chun Zhu, Shibin Tang, Yujun Zuo and Qian Yin

Received: 10 July 2024
Revised: 22 August 2024
Accepted: 29 August 2024
Published: 3 September 2024

1. Introduction

Underground mining operations lead to a disturbance of the initial structure of the strata. This is related to the disturbance of stresses in the rock mass, which may lead to an increase in seismic activity or the occurrence of rock outbursts in the area of exploitation [1]. Additionally, as a result of underground mining operation, deformations are created on the ground surface, which can lead to so-called mining damage. This problem has been the subject of numerous scientific studies conducted around the world since the 19th century. However, the greatest development of modelling and computational methods and their modifications occurred in 1950–1990. The methods of that time focused on analytical solutions: geometric-integral and stochastic. Their advantages and disadvantages were described in many works. An example of such analyses conducted for the Knothe method [2,3], which is one of the most popular geometric-integral methods used in science and mining industry, are the experiments described by [4–10], among others. As can be noticed, the topic of using analytical methods to predict ground deformation is still popular despite the passage of years, and research is being conducted on adapting methods and parameters to mining and geological conditions [11]. These methods owe their popularity to the ease of conducting analyses for a large number of exploitation fields and obtaining quick forecast results. However, the effectiveness of forecasts based on these methods depends on the complexity of the geological structure of the region, including tectonic disturbances of the rock mass and the occurrence of layer packages with different mechanical properties.

Meanwhile, in parallel, since the 1990s, there has been a significant increase in interest in using solutions based on numerical methods [12–14] to determine changes in the state of stress and strain of the rock mass caused by underground mining operations. The authors of these solutions used a variety of numerical methods and physical and mathematical models [15–17]. These methods allow taking into account many additional factors affecting the nature and development of surface deformation [12,18–23], which is largely an advantage over classical computational methods. However, attention should also be paid to the problems that occur during rock mass modelling. One of the main problems, in addition to the selection of the material law and the size of the model, the density of the elements, and the compensation of numerical disturbances, is the proper calibration of the mechanical parameters of the rock layers. The first work on this topic was based on mapping the rock mass with isotropic elastic models [24–26], which, however, due to their nature, showed the correctness of the subsidence trough calculations only in terms of the vertical displacement index. A further attempt to use elastic models modified in terms of not transferring tensile stresses by the modeled elements to predict land sur-face deformations in the mining area was conducted by Chrzanowska-Szostak [27]. She used these elements for the weakening zone whose geometry was determined a priori. Some scientists used elastic–plastic models to describe the impact of exploitation on the surface. Adopting this model in a physical sense has greater understanding because rocks exhibit elastic properties only to a very small extent. However, studies conducted by Siriwardane [28], Whittaker and Reddish [29], Najjar and Zaman [13], and Derbin [30] showed that the modeled subsidence trough has a much larger extent than indicated by surface observations. In parallel, work was carried out on the use of transversally isotropic models to analyze the impact of exploitation on the land surface. In 1964, Berry [31] was the first to notice the advantages of using this type of models to limit the width of the modeled trough. Further research presented by Hazine [25] and McNabb [32] confirmed the validity of the adopted model. In 2019, Derbin [33] conducted analyses for several constitutive models: Mohr–Coulomb and modified Hoek–Brown. They confirmed the research results of their predecessors that elastic–plastic models overestimate the width of the subsidence trough. A similar conclusion was presented after using the Clay and Sand Model or CASM models [30]. Further work is mainly related to combining continuous and discontinuous numerical methods in order to obtain satisfactory results of deformation indicators, including Vyazmensky [34], Zhang [35], or the work of Liu [36], and Li [37]. Another important problem concerns the selection of parameter values for the adopted model. This issue was the subject of separate studies, and their results have been presented in various articles, among others [16,22,38–40]. Further development of numerical methods on the issue of land surface deformations resulting from underground mining works made it possible to use them to analyze this phenomenon regardless of the nature and cause of the deformation, including strip pillar exploitation [41], underground coal gasification [42], land uplift when flooding underground mines [43–46], determining their impact on surface objects [47].

In this article, the authors initially used the methodology for estimating the geomechanical parameters of rock layers developed by Tajduś [39], which was optimized for the advancing mining front, based on the author's Python script-based program. In addition, a modification related to the evaluation of the error of estimated parameter values described in this article was introduced in the program. Numerical analyses were carried out for a selected region of the Piast–Ziemowit mine (Poland) using both mining, geological and geodetic data.

2. Materials and Methods

2.1. Area of Interest

The research area covers the city and commune of Lędziny located in the Upper Silesian Coal Basin (USCB) in southern Poland, in the mining area of the Piast–Ziemowit coal mine belonging to Polish Mining Group Company (Figure 1). The research area covers an area of approximately 2 km^2. The development of the area is dominated by single-

family residential buildings supplemented with agricultural, forest and industrial areas. Underground hard coal exploitation in Lędziny began at the end of the 19th century. In total, 5 coal seams at a depth of 50 to 320 m were mined in the analyzed region. The last, fifth coal seam was exploited at the end of the 1970s. The analyzed mining works were carried out on seam 215, which lies almost horizontally at a depth of 420 m.

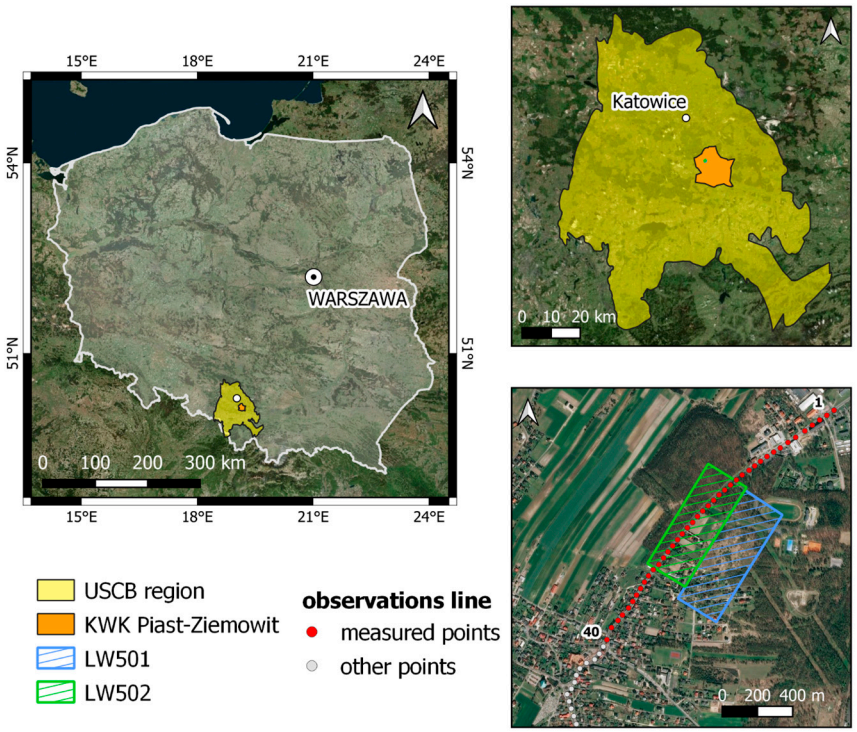

Figure 1. Area of Interests (AOI) localization with the scheme of observation points and exploitation of coal longwalls LW501 and LW502 in seam 215.

This article presents the results of research on the impact of exploitation two coal longwalls LW501 and LW502 on the land surface (Figure 1). Exploitation was carried out in a longwall system with roof collapse. The average height of exploitation was 1.9 m. The LW501 longwall with dimensions 570 × 200 (meters, length and width) was exploited in the period from June to December 2021. And then, the LW502 longwall with a 520 m long and 200 m width run was exploited in the period from December 2021 to end of May 2022.

The rock mass in the analyzed region is characterized by the presence of Carboniferous rocks represented by sedimentary series of sandstone, conglomerates, and shale with deposits of hard coal adhering to the upper Carboniferous. Carboniferous layers are found under the cover of younger origin, i.e., Triassic, Miocene, and Quaternary deposits. Quaternary sediments are represented by the Pleistocene and Holocene deposits, mainly moraine clays as well as dust, sand, and gravel. The Triassic formations are mainly made up of Lower Triassic sandstones, siltstones and claystones, dolomites and marls. Subsequent coal seams are located between thick layers of sandstone, which are between 35 and 100 m thick. Directly above seam 215, there is a 100 m-thick sandstone layer with interfacing in the form of clays and conglomerates. There is a 70 m-thick sandstone layer on the floor.

2.2. Levelling and GNSS Measurements

In the AOI, there is an observation line that is 4250 m long. It extends north-east to south-west approximately along the longitudinal axis of the LW502 longwall (Figure 1). It consists of 114 observation points permanently stabilized in the ground.

Due to the expected range of revealing mining influences, geodetic observations were carried out on the section from point No. 1 in the north to point No. 40 in the south

(red points in Figure 1) from June 2021 to August 2022. During this period, the mine's measuring department performed 5 series of geometric levelling measurements (the dates of the measurements are listed in Table 1). The levelling measurements were related to the three reference benchmarks of the GIGANT levelling network, which are beyond the range of the mining exploitation influence, and the heights of the points were determined in the PL-EVRF2007-NH altitude system. Height measurements were carried out using a Leica LS15 level using carbon fiber code staffs. The average error m_H in determining the height of the observation line measurement points is $m_H \leq 0.015$ m. Levelling measurements were supplemented with independent satellite measurements with a GNSS receiver. Satellite observations were made in August 2022 with Spectra Precision SP60 receiver in the GNSS RTN technology, using correction corrections from the national system of ASG-EUPOS reference stations. The coordinates of the points were determined in the PUWG2000 zone 6 system (Poland CS2000 zone 6; PL-EVRF89-2000, EPSG: 2177) and the PL-EVRF2007-NH altitude system. The average error in determining the position of points using the ASG-EUPOS system corrections is $m_{XY} < \pm 0.03$ m in the horizontal plane and $m_H < \pm 0.05$ m for the height [48].

Table 1. Dates of geodetic measurements: levelling and GNSS.

Date of Measurements dd/mm/yyyy	
Leveling	**GNSS**
7 June 2021	
28 September 2021	
25 November 2021	
11 March 2022	
12 May 2022	4 August 2022

2.3. Finite Element Method Simulation

Based on many years of authors experience as well as on the basis of literature analysis, the transversally isotropic model is the most reflecting constitutive model of the rock mass. Research conducted over many years has proven that rocks have anisotropic properties [26,49–52]. In 1970, Tremmel and Widmann [53] conducted laboratory studies to determine the value and nature of shale anisotropy. They cut samples from the rock block in six different directions and subjected them to a uniaxial compression test. As a result of the research carried out in this way, they found that the anisotropy of rocks increases with the increase in the acting load and that it is possible to adopt a simple anisotropy model with nine constants of the type: E_1, E_2, E_3, G_{12}, G_{23}, G_{31}, ν_{12}, ν_{13}, ν_{23} called the orthotropic model. Similar studies on the orthotropy of rocks were carried out by Nishimatsu [54] examining the behavior of the Mesozoic shale and [55]. As a result of these studies, they concluded that it is possible to adopt an anisotropic model with five elastic constants called the anisotropic axisymmetric model (transversally isotropic model in Figure 2).

Anisotropic properties can be caused by both geological processes during rock formation and subsequent tectonic processes, as well as processes resulting from human activity (anisotropy of rocks resulting from cracks resulting from exploitation). Research on the anisotropy of mechanical properties of rocks was carried out, among others, by Lepper [56], Akai [57], Allirot and Bocher [58], Szwilski [59], and Gustkiewicz [60]. The most important conclusions from the research on rock anisotropy indicate:

- Sedimentary rocks have anisotropic properties,
- In most cases:
    - The elastic modulus perpendicular to the lamination is greater than the modulus of elasticity parallel to the lamination,
    - The strength of the rock in the direction perpendicular to the interleaving plane is greater than in the direction parallel,

- Due to the simplicity of describing the behavior of such rocks, it is possible to adopt an anisotropic model with five elastic constants.

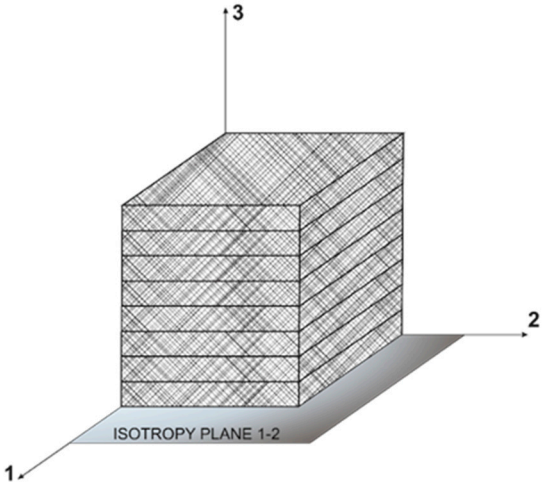

Figure 2. The diagram of the transversally isotropic model.

In transversally isotropic model, assuming the isotropy plane in directions 1–2, the modulus of elasticity is defined as follows: $E_1 = E_2$, E_3, $\nu = \nu_{12} = \nu_{13} = \nu_{23}$, G_{13}. Additionally, the modulus of shear elasticity in the isotropy plane G_{12} can be distinguished, calculated from the formula:

$$G_{12} = \frac{E_1}{2 \cdot (1 + \nu_{12})} \quad (1)$$

When there is no laboratory data on the value of the G_{13} form elasticity parameter, the formula developed by Lekhnitskii [61] can be used:

$$G_{13} = \frac{E_1 \cdot E_3}{E_1 \cdot (1 + 2 \cdot \nu) + E_3} \quad (2)$$

Numerical modelling of the impact of underground mining on the land surface using a transversely isotropic model was presented, among others, by Walaszczyk [62], Thin, Pine and Trueman [63], Mielimąka and Wesołowski [64] and Tajduś [19,39].

Based on the abovementioned literature analysis and the experience concerning numerical modelling of underground hard coal mining, it was decided to use the transversally isotropic model in numerical analyses. The initial parameters for iterative procedure were estimated on the basis of the results of strength tests of rock samples (Table 2) and the methodology presented in the work by Tajduś [39].

Table 2. Geomechanical properties of the seam 215 and surrounding rocks.

	R_c [MPa]		R_r [MPa]	Roof and Floor Class
	Average	Range		
Roof	24.2	14.6–37.5	2.4	III [1]
Coal	32.9	20.1–44.2	–	–
Floor	24.7	24.1–27.3	–	II [2]

[1] Class III means that the direct ceiling is made of rigid rocks, difficult to process, or above the coal seam, there is a roof consisting of a thick layer of strong rocks. [2] Class II means that the direct floor is made of strong rock layers.

The initial values of elastic modulus E_m of transversally isotropic model for the rock mass layers using Hoek's rock mass classifications [65] and the strength values of the laboratory parameters of the rock samples were estimated based on formulas (Equations (3) and (4)) as follows [66,67]:

- For $R_c \leq 100$ MPa:

$$E_m = \left(1 - \frac{D}{2}\right) \cdot \sqrt{\frac{R_c}{100}}\, 10^{\frac{GSI-10}{40}} \quad (3)$$

- For $R_c > 100$ MPa:

$$E_m = \left(1 - \frac{D}{2}\right) \cdot 10^{\frac{GSI-10}{40}} \quad (4)$$

where:
R_c—the uniaxial compressive strength of intact rock material, which provides a system for estimating the reduction in rock mass strength for different geological conditions (Table 2).
GSI—value of the geological strength index for the rock mass [65],
D—the degree of disturbance, to which the rock mass has been subjected by blast damage and stress relaxation [67].

Based on geological data from a borehole (Table 3) 3D numerical model of AOI was prepared (Figure 3). The dimension of the 3D model was 3420 × 2780 × 600 m. The model was constructed using hexahedral (hex) elements, with a total number of elements close to 3,000,000. In the area of the longwall panel, the element size was set to 1 m. From the edges of the longwall panel to the model boundaries, a bias was used, resulting in element sizes ranging from 0.5 m to 10 m. In the vertical direction (z-direction), the element size was consistently set to 1 m.

Table 3. Geological characterization of the mining area used in numerical simulations.

No.	Stratum	Layer's Floor Depth [m]	Thickness [m]
1	Quaternary	10	10
2	Sandstone	185	175
3	Siltstone	200	15
4	Sandstone	240	40
5	Siltstone	275	35
6	Sandstone	300	25
7	Siltstone	320	20
8	Sandstone	418	98
9	Coal	420	2
10	Sandstone	600	180

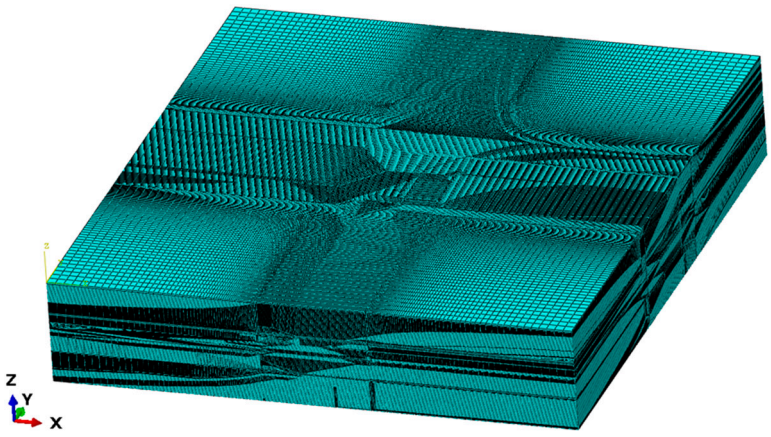

Figure 3. Numerical model of AOI.

These sizes were chosen to balance computational efficiency with the accuracy required to capture the deformation behavior accurately.

The geometric conditions for each longwall were as follows:

- LW501—200 m width, 570 m long, 1.90 m high and with a 8 m caving zone;

- LW502—200 m width, 520 m long, 1.90 m high and with a 8 m caving zone.

Numerical calculations were carried out for three-dimensional models in two steps (Figure 4), which were simulation of:

1. Initial state of stress and strain,
2. Coal extraction with roof collapse—for this purpose, so-called equivalent elements with reduced parameter values in the highly disturbed mining zone (cave-in zone) were implemented.

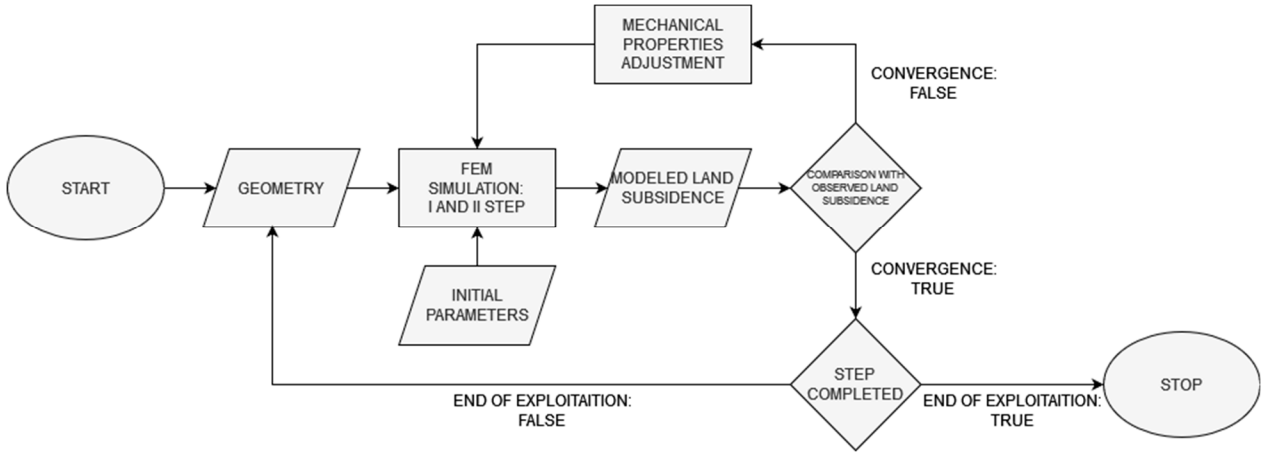

Figure 4. The procedure of optimization rock layers parameters.

Results of initial parameters for the analyzed region of KWK Piast—Ziemowit mine were compiled in Table 4.

Table 4. Initial mechanical parameters of rock mass layers.

	G_{12} [GPa]	G_{13} [GPa]	G_{23} [GPa]	E_1 [GPa]	E_2 [GPa]	E_3 [GPa]	$\upsilon_{12} = \upsilon_{13} = \upsilon_{23}$
Quaternary	0.02	0.04	0.04	0.04	0.04	0.68	0.15
Sandstone	0.35	0.74	0.74	0.80	0.80	13.33	0.15
Siltstone	0.16	0.35	0.35	0.38	0.38	6.32	0.15
Caves zone	-	-	-	-	-	0.0188 *	0.30
Coal	0.22	0.48	0.48	0.51	0.51	8.57	0.15

* Assumed elastic isotropic model. Values calculated according to Tajduś [39].

Changes in the values of rock layer parameters were made with the assumption of a constant change coefficient for all rock layers. It was determined as the ratio of the Young's modulus in the vertical direction of the rock layers specified for a given advancement of the face (E_3^{adv}) to the value of the modulus before the commencement of exploitation (E_3^{init}) determined from laboratory tests (assumed as an initial parameter for calculations):

$$X = \frac{E_3^{adv}}{E_3^{init}} \tag{5}$$

The values of the elasticity moduli for the caving zone were determined according to Tajduś [39] and were considered constant for all advancements of the exploitation face.

In the presented method, the Nelder–Mead algorithm is used as a method to optimize the search for the minimum of a function [68,69]. This approach does not require the computation of gradients, making it suitable for functions that are noisy or have discontinuities. Operational boundary parameters and laboratory parameters of geomechanical rock layers are required as input data, as initial parameters of the rock mass. The objective function was

defined as the RMSE error value, which allows comparison of the simulated subsidence with the results of geodetic observations.

As a result of performed calculations, the distribution of land surface displacements has been received for each face advance along with adjusted mechanical parameters of rock layers to the current mining situation.

2.4. Numerical Modeling Evaluation Based on Geodetic Measurement

The accuracy of the FEM modelling of subsidence can be assessed on the basis of various error measures [5,70]:

- Mean error:

$$\mathrm{ME} = \frac{\sum\left(s^{i}_{obs} - s^{i}_{FEM}\right)}{n} \tag{6}$$

where:
s^{i}_{obs}—observed subsidence of i-th observation point,
s^{i}_{FEM}—FEM simulated subsidence of i-th observation point, and
n—number of observation points.

- Mean absolute error:

$$\mathrm{MAE} = \frac{\sum\left(\left|s^{i}_{obs} - s^{i}_{FEM}\right|\right)}{n} \tag{7}$$

- Root mean squared error:

$$\mathrm{RMSE} = \sqrt{\frac{\sum\left(s^{i}_{obs} - s^{i}_{FEM}\right)^{2}}{n}} \tag{8}$$

- Percent error for maximum subsidence:

$$\mu_{s_{max}} = \frac{s^{obs}_{max} - s^{FEM}_{max}}{s^{obs}_{max}} \cdot 100\% \tag{9}$$

where:
s^{obs}_{max}—maximum value of observed subsidence;
s^{mod}_{max}—maximum value of FEM simulated subsidence.

The accuracy measures expressed by the Formulas (6)–(8) determine the average error s_{FEM} of a single point from the entire profile. These measures are very susceptible to the occurrence of systematic errors caused by the presence of the operating rim (horizontal shift of the subsidence trough profile). Successive measures expressed by Formula (9) indicate the percentage error of the modeled subsidence. They describe the relative errors, i.e., in relation to the maximum subsidence values s^{obs}_{max}.

3. Results of Conducted FEM Simulations for LW501 and LW502 Longwall Panels Exploitation

The development of the subsidence trough, observable on the observation line during the operation of the LW501 and LW502 longwalls, is presented in Figure 5. Due to the significant distance of the observation line points from the operation carried out from June to December 2021, i.e., the LW501 longwall, the recorded subsidence does not exceed 4 cm at the end of November 2021. Only the exploitation of the LW502 longwall carried out directly under the observation line leads to larger displacements of the terrain surface. Exploitation was carried out in direction from point 40 to point 1, which shows the development of the subsidence trough in Figure 5. The operation was completed at the end of May 2022, and a slight increase in subsidence between the last two observation series (12 May 2022 and 4 August 2022) indicates the presence of residual subsidence on the land surface. The maximum observed subsidence on the observation line equals $s^{obs}_{max} = 661$ mm at point 23.

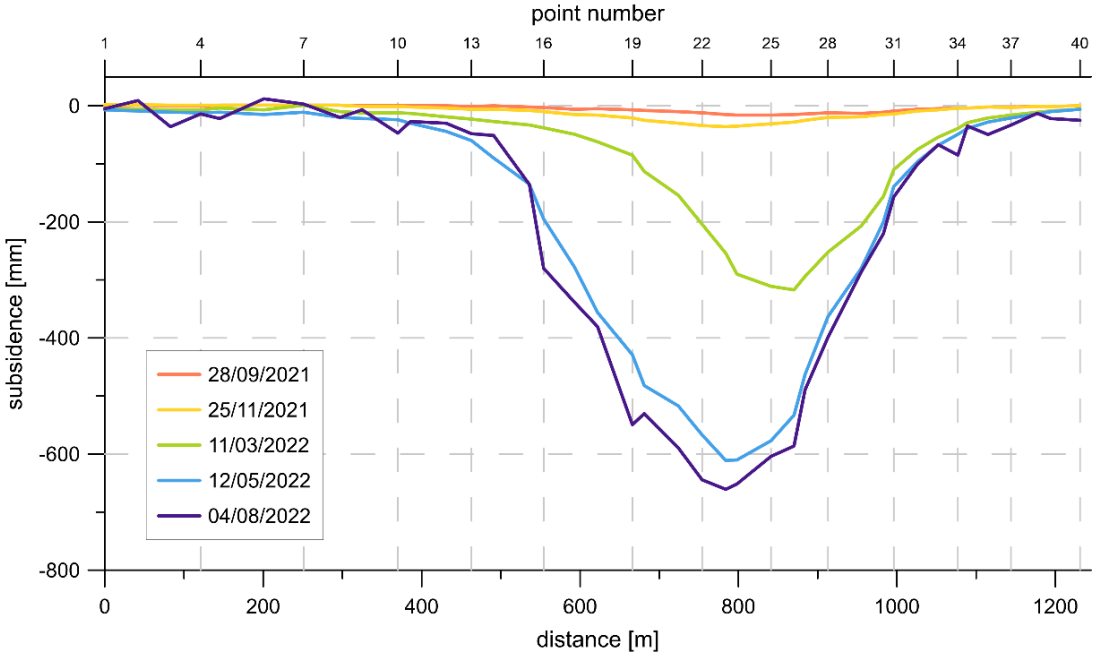

Figure 5. Land surface subsidence along the observation line.

The second series of land surface subsidence measurements were carried out at the end of November 2021. As of this day, the face advance of longwall panel 501 was determined at a distance of 500 m from the beginning of the longwall. The maximum measured subsidence was 36 mm and it was located in point no. 23. Having this information, the parameters of the rock layers were calibrated using ABAQUS 2022 hf4 software and author's Python 3.9 script in order to adjust the simulated subsidence to the real values. The estimated values of mechanical parameters are listed in Table 5 and the plot of fit is shown in Figure 6.

Table 5. Final mechanical parameters of rock mass layers—mining situation—25 November 2021.

	G_{12} [GPa]	G_{13} [GPa]	G_{23} [GPa]	E_1 [GPa]	E_2 [GPa]	E_3 [GPa]	$v_{12} = v_{13} = v_{23}$
Quaternary	0.01	0.02	0.02	0.02	0.02	0.41	0.15
Sandstone	0.10	0.21	0.21	0.23	0.23	3.79	0.15
Siltstone	0.21	0.45	0.45	0.48	0.48	8.00	0.15
Coal	0.13	0.29	0.29	0.31	0.31	5.14	0.15

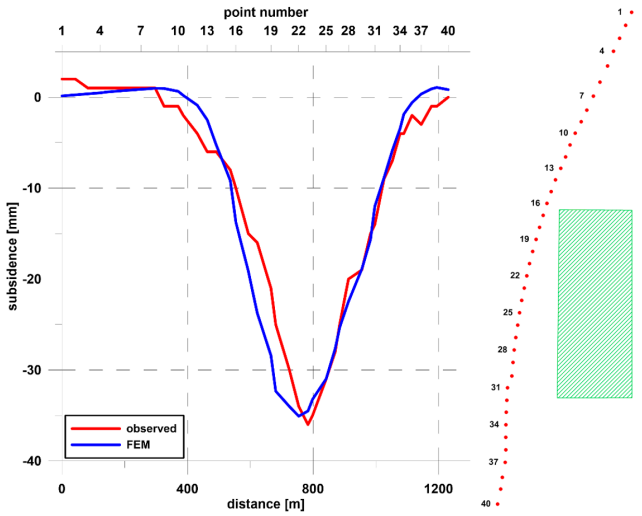

Figure 6. Comparison of the observed and simulated subsidence—25 November 2021.

In Figure 7, the distribution of land surface subsidence based on FEM analysis is shown. For the analyzed mining situation, the maximum subsidence of 433 mm was obtained.

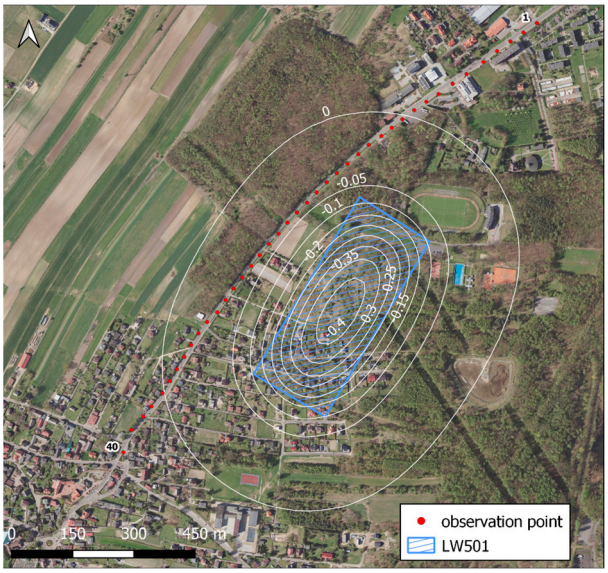

Figure 7. Land surface subsidence (in meters) based on FEM analysis—25 November 2021.

The fifth series of land surface subsidence measurements were carried out at the beginning of August 2022. As of this day, the mining of the longwall panel 501 and 502 have been completed. The maximum measured subsidence was 637 mm and it was located in point no. 23. Having this information, the parameters of the rock layers were calibrated using Abaqus software and Python script in order to adjust the simulated subsidence to the real values. The estimated values of mechanical parameters are listed in Table 6 and the plot of fit is shown in Figure 8.

Table 6. Final mechanical parameters of rock mass layers—mining situation—4 August 2022.

	G_{12} [GPa]	G_{13} [GPa]	G_{23} [GPa]	E_1 [GPa]	E_2 [GPa]	E_3 [GPa]	$v_{12} = v_{13} = v_{23}$
Quaternary	0.02	0.03	0.03	0.04	0.04	0.61	0.15
Sandstone	0.15	0.32	0.32	0.34	0.34	5.69	0.15
Siltstone	0.31	0.67	0.67	0.72	0.72	12.00	0.15
Coal	0.20	0.43	0.43	0.46	0.46	7.71	0.15

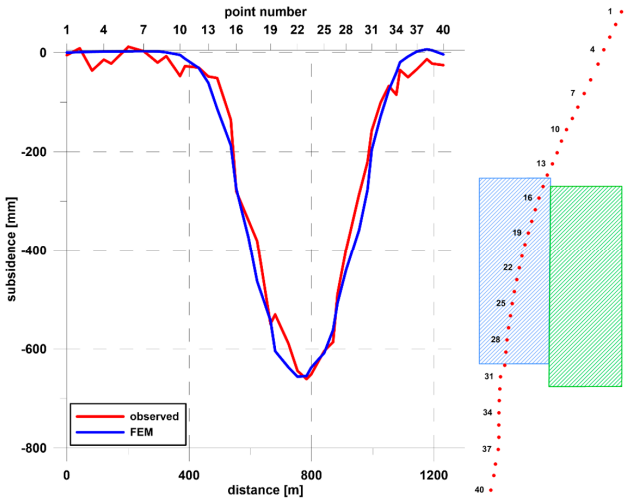

Figure 8. Comparison of the observed and simulated subsidence—4 August 2022.

In Figure 9, the distribution of land surface subsidence based on FEM analysis is shown. For the analyzed mining situation the maximum subsidence of 917 mm was obtained.

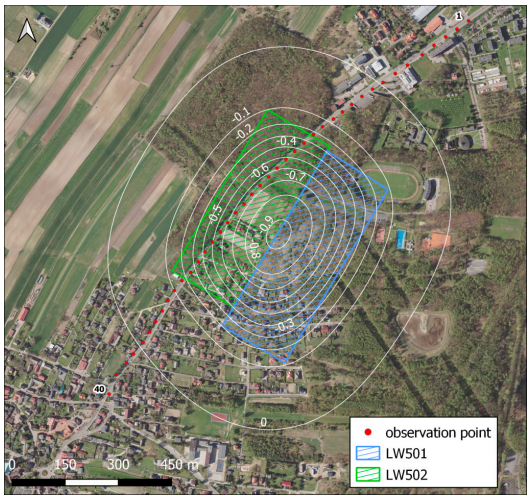

Figure 9. Land surface subsidence (in meters) based on FEM analysis—4 August 2022.

The obtained error values (see chapter 2.4) of numerical modelling (Table 7) indicate the correct determination of the deformation model parameters. Positive ME values mean an average underestimation of the subsidence, while negative values mean higher modelled values in relation to the observed subsidence. The increase in the absolute error values (MAE, RMSE) from 1 to 35 mm for successive states of exploitation is related to the development of the trough and the occurrence of subsidence in the range of exploitation impact. The percent error for maximum subsidence $\mu_{s_{max}}$ describes the accuracy of determining the maximum subsidence. Its value does not exceed 2.6% · s_{max}^{obs}.

Table 7. Modeling subsidence errors with the numerical method for subsequent face advances.

	28 September 2021	25 November 2021	11 March 2022	12 May 2022	4 August 2022
ME [mm]	−0.5	0.3	−7.1	3.1	5.7
MAE [mm]	0.9	2.0	18.0	23.7	27.4
RMSE [mm]	1.1	2.8	22.1	30.0	34.7
$\mu_{s_{max}}$ [%]	2.3	2.6	0.5	−1.7	0.7

4. Discussion

As part of the conducted analyses, numerical calculations were performed to assess the impact of the ongoing mining exploration of the KWK Piast–Ziemowit mine in panels LW501 and LW502 on surface deformation. The calculations were carried out using a custom script based on Python, which allows for the automatic estimation of the values of parameters of the modelled rock layers located above the formed caving zone. To ensure the clarity of the results, the parameter values in the caving zone were assumed to be constant for all numerical models. This assumption does not align with observations of the behavior of caving zones resulting from mining activities. Previous studies unequivocally indicate that as mining progresses, the caving zone increases in height, causing various rock strata to collapse. Unfortunately, this assumption was necessary to ensure the clarity of the solution based on a program that automatically determines the mechanical parameters of individual rock layers. The program performed calculations according to the specified conditions and then compared the estimated deformation indicators with the measured values. The results are presented for a selected region of the underground coal mine. However, the methodology used allows for the determination of deformation indicators and rock mass parameters also for other regions of the mine. It is limited only by knowledge of mining conditions and having geodetic measurements and geological structure with preliminary

parameters. Based on these data, the program will adjust the values of "real" parameters to the measurement results using the method of similarity of geode measurement results described in this article. According to the procedure, calculations were conducted until the consistency of the selected deformation indicators was achieved, i.e., obtaining the global minimum of the specified objective function, which was the RMSE error. Subsequently, calculations were carried out for the next specified mining advance.

The calculations showed a very high consistency of deformation indicators (see Table 7), meaning that for the assumed physical model, the actual values of the mechanical parameters of the rock layers were determined with high probability. Another way to assess accuracy of numerical modelling result is another deformation indicator. Based on the field observation data the tilts of subsidence trough profile were compared. The fitting errors of the modelled inclination T_{FEM} were determined in relation to the measured values T_{obs} similarly to those for subsidence, in accordance with Formulas (6)–(9). The results for individual operating states are presented in Table 8.

Table 8. Modeling tilt errors with the numerical method for subsequent face advances.

	28 September 2021	25 November 2021	11 March 2022	12 May 2022	4 August 2022
ME [mm/m]	0.00	0.00	0.00	−0.01	−0.04
MAE [mm/m]	0.03	0.06	0.23	0.38	0.97
RMSE [mm/m]	0.04	0.07	0.38	0.56	1.21
$\mu_{S_{max}}$ [%]	−10.2	−3.2	−14.6	−13.8	29.5

Similarly to the subsidence, Figure 10 shows the tilts profiles of the subsidence trough after the end of operation of the LW 501 and LW502 walls.

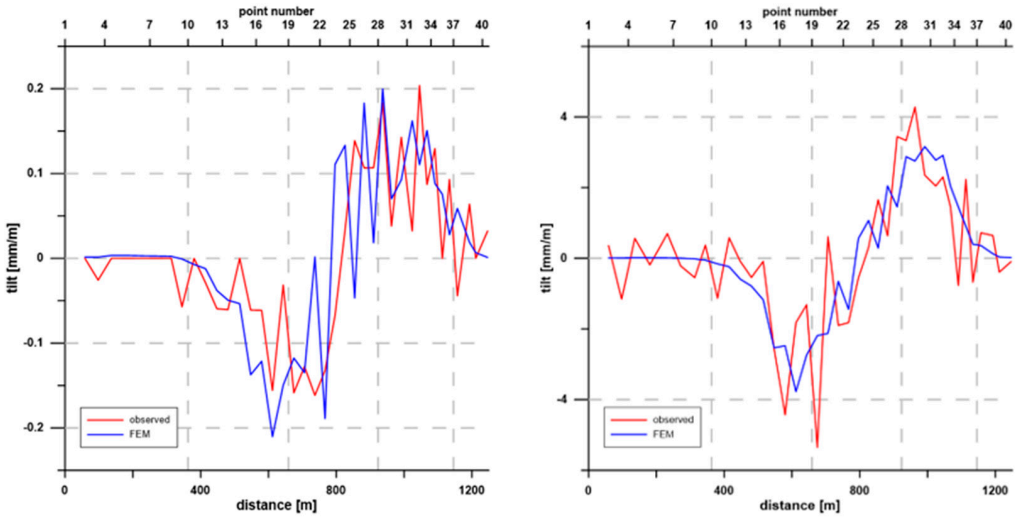

Figure 10. Comparison of the observed and simulated tilts—25 November 2021 (**left**) and 4 August 2022 (**right**).

The obtained results indicate a good and very good match of the tilts of the subsidence trough. The increased fluctuations in relation to the subsidence result from the nature of the phenomenon, which was confirmed on the basis of research on the variability of deformation indicators and forecasting accuracy in numerous publications (e.g., [71]).

The last period (4 August 2022) is characterized by increased values of error characteristics compared to the previous ones (see Table 8). The reasons for this state of affairs should be sought primarily in the measurement technology used to determine the subsidence in observation points. For this purpose, the results of RTN-GNSS measurements were used (see Section 2.2), which are characterized by a much larger error in determining the height ($m_H < \pm 0.05$) compared to the heights determined based on geometric levelling ($m_H \leq 0.015$ m).

The mechanical parameters, particularly the ratio E1/E3, played a crucial role in the accuracy of the numerical models. This ratio, which compares the horizontal Young's modulus (E1) to the vertical Young's modulus (E3), is essential in determining the anisotropic behavior of rock layers. Anisotropy in rock mechanics refers to the directional dependence of rock properties, and the E1/E3 ratio is a key indicator of this behavior. It is also responsible for the change in the slope within the subsidence trough, while Young's modulus (E3) influences the value of land surface subsidence. Poisson's number causing a slight change in subsidence trough course [72]. Recent studies have highlighted the impact of anisotropy on rock deformation and subsidence predictions. For example, Lekhnitskii's theory on anisotropic elasticity provides a foundation for understanding how the different directional moduli influence stress distribution and deformation in rock masses. In particular, research has shown that the elastic stiffness parameters, including Young's modulus, exhibit strong correlations that significantly affect the rock's response to loading conditions [73]. Additionally, the variation in the E1/E3 ratio influences the deformation characteristics during mining activities. By incorporating the E1/E3 ratio into our numerical models, we achieved high consistency in deformation indicators, which aligns with empirical observations and enhances the reliability of our predictions. This adjustment is crucial for accurately modelling the complex behavior of rock layers under mining-induced stress.

It is noteworthy that high accuracy was also achieved in the case where a full subsidence trough did not form, i.e., for the LW501 panel. As the surface measurements conducted from June 2021 to November 2021 showed, the first panel led to slight surface deformation along the observation line, with a maximum subsidence indicator of 38 mm. The maximum estimated subsidence value was 433 mm in the central part of panel LW501. This most likely means that the extraction of this panel did not lead to the fracture (or breaking) of the thick and strong sandstone layer located directly above the mined seam, which has a thickness of up to 100 m. This assumption is supported by reports on the registration of mining tremors recorded on the surface in the area of Lędziny city (https://grss.gig.eu/en/seismic-map/, accessed on 9 July 2024). From June 2021 to the end of 2022, monitoring stations recorded tremors mainly in the energy magnitude range of $1 \cdot 10^5$J according to the GSIS-2017 scale by $PGVH_{max}$ [74], with the intensity of these tremors classified as the lowest category, i.e., 0.

As is known from engineering experience and the literature on the subject, longwall panels can be classified as sub-critical, critical, and supercritical [75,76]. The critical panel is defined as the width of an extracted panel for which the maximum possible subsidence should occur at one point. The critical width depends upon the geological characteristics of the overburden. In single seam coal mining operations in New South Wales, Australia, the critical value is typically 1–1.6 times the depth of the overburden [38,77]. In Europe (including Germany, Poland, and the Czech Republic) [78] it is estimated that a full subsidence trough will form for an extracted space that meets the condition $d \geq 2R$, where R is the radius of main influence range determined by the formula $R = H \cdot cot\beta$, and d is the shorter dimension of the coal longwall (width or length). This means that the condition for the occurrence of a full subsidence trough is related to the mining depth (H) and the angle of the main influence range (β), whose values should consider the quality and structure of the rock mass. However, describing the rock mass with a single parameter is a challenging task. Therefore, numerical analyses that consider the structure and tectonics of the rock mass allow for a more accurate description of its behavior. As shown by further geodetic measurements, the increase in the exploited area by panel LW502 led to a significant increase in the subsidence indicator (compared to the results obtained for panel LW501). Research carried out so far indicates that in order to properly model the subsidence basin caused by mining, an anisotropic model should be used. Elastic–plastic models are used in the literature. It should be borne in mind that these models allow for high consistency of the modelled subsidence compared to those observed from measurements. However, these models have a big problem with reflecting the range of the main influences *R*. In most cases, this range is obtained as significantly exceeding the values observed in reality

(overestimated). The situation is similar in the case of horizontal displacements, which also deviate significantly from the measured values. The use of an anisotropic model allows to limit the value of R obtained from numerical models. However, it is very difficult to determine all the parameter values describing this model. Therefore, the authors use a simplified transversally isotropic model, which has only 5 parameter values (see Section 2.3). The problems with this model are:

1. Proper selection of parameter values, for this reason the authors used a solution used in science, which allows determining the elastic parameters G_{12} and $G_{13} = G_{23}$, which are difficult to determine for mining conditions.
2. Unfortunately, this model still incorrectly determines the values of horizontal displacements (like other models presented in the literature). Research [79] suggested that the use of contact between the modelled layers allows solving this problem, but these studies did not provide a clear solution (for which layers contact should be used, what friction coefficients should be used, etc.). For this reason, the authors did not take into account the change in friction values and the use of contact between layers in the described tests. Research on this issue will be the subject of further research by the authors.

Further numerical analyses based on FEM and the custom script continued to demonstrate high matching accuracy and allowed the determination of the parameters of the rock layers.

5. Conclusions

This article presents numerical modelling of the advancing mining front at the Piast–Ziemowit mine using Abaqus software and a custom Python script. The research aimed to determine the impact of mining operations on surface displacements and to estimate the mechanical parameters of rock layers. Numerical computation results were compared with geodetic measurements of the surface, verifying the model, and calibrating the mechanical parameters of the rock mass. The presented solution allows for the automation of the process of optimizing the parameters of the adopted geomechanical model. Determining the optimal set of parameters requires finding the minimum of the objective function defined as the RMSE error value. Iterative calculations end when the criterion of convergence of two consecutive simulations is reached. The case study of the Piast–Ziemowit mine was characterized by the presence of a strong rock layer in the rock mass, which prevented the formation of a complete subsidence trough on the surface. Additionally, the dimensions of operation classify it as sub-critical or critical. This means that the observed reductions are smaller than those resulting from empirical formulas for hard coal exploitation. For this reason, the use of numerical modeling for impact calculations for ongoing exploitation requires taking into account changes in the geomechanical properties of the rock mass. This solution is an innovative approach and requires the development of a method for determining them. Nevertheless, the applied numerical modelling method demonstrated high accuracy in predicting surface displacements. The computational results showed good agreement with field measurements, confirming the validity of the model assumptions and the accuracy of the mechanical parameters of the rock layers. It worth to notice, that was also achieved in the case where a full subsidence trough did not form, i.e., for the LW501 panel. This article detailed the calibration process of the numerical model, including methods for error assessment and adjustment of computation results to real measurements. The custom Python script, integrated with Abaqus, enabled automated computation and efficient analysis of large datasets. This facilitated multiple computation iterations in a short time, significantly speeding up the research process.

In conclusion, this study demonstrated that numerical modelling of the advancing mining front using advanced computational tools such as Abaqus and Python script is an effective method for predicting the impact of mining operations on surface displacements. Despite the specific geological conditions of the Piast–Ziemowit mine, this method provided reliable results, confirming its utility in engineering practice.

Author Contributions: Conceptualization, M.D. and K.T.; methodology, M.D. and K.T.; software, M.D.; validation, M.D., D.M. and K.T.; formal analysis, M.D. and D.M.; investigation, K.T.; resources, M.D., D.M. and K.T.; data curation, M.D. and D.M.; writing—original draft preparation, M.D. and D.M.; writing—review and editing D.M., A.S. and K.T.; visualization, M.D. and D.M.; supervision, A.S. and K.T.; project administration, M.D. All authors have read and agreed to the published version of the manuscript.

Funding: This research received no external funding.

Institutional Review Board Statement: Not applicable.

Informed Consent Statement: Not applicable.

Data Availability Statement: The data presented in this study are available on request from the corresponding author. The data are not publicly available due to confidentiality resason.

Acknowledgments: Part of the work in this paper was carried out in 2022 as part of the statutory work of the Strata Mechanics Research Institute of Polish Academy of Sciences in Krakow, financed by the Ministry of Education and Science. We gratefully acknowledge Polish high-performance computing infrastructure PLGrid (HPC Centers: ACK Cyfronet AGH) for providing computer facilities and support within computational grant no. PLG/2023/016419.

Conflicts of Interest: The authors declare no conflicts of interest.

References

1. Li, X.; Chen, D.; Fu, J.; Liu, S.; Geng, X. Construction and Application of Fuzzy Comprehensive Evaluation Model for Rockburst Based on Microseismic Monitoring. *Appl. Sci.* **2023**, *13*, 12013. [CrossRef]
2. Knothe, S. A Profile Equation for a Definitely Shaped Subsidence Trough (Równanie Profilu Ostatecznie Wykształconej Niecki Osiadania). *Arch. Górnictwa Hut.* **1953**, *1*, 22–38.
3. Knothe, S. *Prediction of Mining Influence*; Śląsk Publishing House: Katowice, Poland, 1984. (In Polish)
4. Chi, S.; Wang, L.; Yu, X.; Lv, W.; Fang, X. Research on Dynamic Prediction Model of Surface Subsidence in Mining Areas with Thick Unconsolidated Layers. *Energy Explor. Exploit.* **2021**, *39*, 927–943. [CrossRef]
5. Gruszczyński, W.; Niedojadło, Z.; Mrocheń, D. Influence of Model Parameter Uncertainties on Forecasted Subsidence. *Acta Geodyn. Geomater.* **2018**, *15*, 211–228. [CrossRef]
6. Guo, X.W.; Yang, X.Q.; Chai, S.W. Optimization of the Segmented Knothe Function and Its Dynamic Parameter Calculation. *Rock Soil Mech.* **2020**, *41*, 2091–2097+2109. [CrossRef]
7. Karmis, M.; Agioutantis, Z.; Jarosz, A. Recent Developments in the Application of the Influence Function Method for Ground Movement Predictions in the U.S. *Min. Sci. Technol.* **1990**, *10*, 233–245. [CrossRef]
8. Jiang, Y.; Misa, R.; Tajduś, K.; Sroka, A.; Jiang, Y. A New Prediction Model of Surface Subsidence with Cauchy Distribution in the Coal Mine of Thick Topsoil Condition. *Arch. Min. Sci.* **2020**, *65*, 147–158. [CrossRef]
9. Hu, Q.; Deng, X.; Feng, R.; Li, C.; Wang, X.; Jiang, T. Model for Calculating the Parameter of the Knothe Time Function Based on Angle of Full Subsidence. *Int. J. Rock Mech. Min. Sci.* **2015**, *78*, 19–26. [CrossRef]
10. Sroka, A. *Zeiträumliche Lösung der Theorie von Knothe*; Geodäsie Heft 24; Polnische Akademie der Wissenschaften: Krakau, Poland, 1978.
11. Niedojadło, Z.; Gruszczyński, W. The Impact of the Estimation of the Parameters Values on the Accuracy of Predicting the Impacts of Mining Exploitation. *Arch. Min. Sci.* **2015**, *60*, 173–193. [CrossRef]
12. Alejano, L.R.; Ramírez-Oyanguren, P.; Taboada, J. FDM Predictive Methodology for Subsidence Due to Flat and Inclined Coal Seam Mining. *Int. J. Rock Mech. Min. Sci.* **1999**, *36*, 475–491. [CrossRef]
13. Najjar, Y.; Zaman, M. Numerical Modeling of Ground Subsidence Due to Mining. *Int. J. Rock Mech. Min. Sci. Geomech. Abstr.* **1993**, *30*, 1445–1448. [CrossRef]
14. Afsarl, N.; Reddish, D.J. Numerical Modelling of Surface Subsidence Arising from Longwall Mining of Steeply Inclined Coal Seams. In Proceedings of the II'h Turkish Coal Congress, Bartm-Amsara, Turkey, 10–12 June 1998; pp. 53–64.
15. Liu, S.; Li, K.; Shi, W.; Wang, Z.; Zhang, H.; Li, Z. Analysis of Mining Subsidence Characteristics and Deformation Prediction Considering Size Parameters and Mechanical Parameters. *Geofluids* **2022**, *2022*, 5495509. [CrossRef]
16. Li, H.; Zha, J.; Guo, G. A New Dynamic Prediction Method for Surface Subsidence Based on Numerical Model Parameter Sensitivity. *J. Clean. Prod.* **2019**, *233*, 1418–1424. [CrossRef]
17. Tajduś, K.; Sroka, A.; Tajduś, A.; Preusse, A. Three Dimensional Modeling of a Surface Displacements as a Result of an Underground Longwall Panel Extraction. In Proceedings of the 29th International Conference on Ground Control in Mining, Morgantown, VA, USA, 27–29 July 2010.
18. Fathi Salmi, E.; Nazem, M.; Karakus, M. Numerical Analysis of a Large Landslide Induced by Coal Mining Subsidence. *Eng. Geol.* **2017**, *217*, 141–152. [CrossRef]

19. Tajduś, K. Numerical Simulation of Underground Mining Exploitation Influence upon Terrain Surface. *Arch. Min. Sci.* **2013**, *58*, 605–616.
20. Sainsbury, B.-A. A Model for Cave Propagation and Subsidence Assessment in Jointed Rock Masses. Ph.D. Thesis, UNSW Sydney, Sydney, Australia, 2012.
21. Malinowska, A.A.; Misa, R.; Tajduś, K. Geomechanical Modeling of Subsidence Related Strains Causing Earth Fissures. *Acta Geodyn. Geomater.* **2018**, *15*, 197–204. [CrossRef]
22. Shu, J.; Jiang, L.; Kong, P.; Wang, P.; Zhang, P. Numerical Modeling Approach on Mining-Induced Strata Structural Behavior by Considering the Fracture-Weakening Effect on Rock Mass. *Appl. Sci.* **2019**, *9*, 1832. [CrossRef]
23. Tajduś, K.; Sroka, A. Analytic and Numerical Methods of Sinkhole Prognosis. In Proceedings of the 7th Altbergbau Kolloquium, Freiberg, Germany, 11–13 October 2023; Verlag Glückauf GmbH: Freiberg, Germany, 2007; pp. 152–165.
24. Shippman, G.K. *Numerical Investigation of Elastic Behaviour around Longwall Excavations*; University of Nottingham: Nottingham, UK, 1975.
25. Hazine, H.I. *A Study of the Development of Surface Strains Produced by Mining*; University of Nottingham: Nottingham, UK, 1977.
26. Salamon, M.D.G. Two-Dimensial Treatment of Problems Arising from Mining Tabular Deposits in Isotropic or Transversaly Isotropic Ground. *Int. J. Rock Mech. Sci. Geomech. Abstr.* **1968**, *5*, 159–185. [CrossRef]
27. Chrzanowska-Szostak, A.; Chrzanowski, A.; Massiera, M. Use of Geodetic Monitoring Measurements in Solving Geomechanical Problems in Structural and Mining Engineering. In Proceedings of the 11th FIG Symposium on Deformation Measurements, Santorini, Greece, 25–28 May 2003.
28. Siriwardane, H.J. A Numerical Procedure for Prediction of Subsidence Caused by Longwall Mining. In Proceedings of the 5th International Conference on Numerical Methods in Geomechanics, Nagoya, Japan, 1–5 April 1985.
29. Reddish, D.J.; Whittaker, B.N. *Subsidence: Occurrence, Prediction and Control*; Elsevier Science: Amsterdam, The Netherlands, 2012; ISBN 9780444598349.
30. Derbin, Y.; Walker, J.; Wanatowski, D.; Marshall, A.M. Implementation of Advanced Constitutive Models for the Prediction of Surface Subsidence after Underground Mineral Extraction. In *Proceedings of China-Europe Conference on Geotechnical Engineering*; Wu, W., Yu, H.-S., Eds.; Springer International Publishing: Cham, Switzerland, 2018; pp. 320–323.
31. Berry, D.S. The Ground Considered as a Transversely Isotropic Material. *Int. J. Rock Mech. Min. Sci. Geomech. Abstr.* **1964**, *1*, 159–167. [CrossRef]
32. McNabb, K.E. *Three Dimensional Numerical Modeling of Surface Subsidence Induced by Underground Mining*; The University of New South Wales: Sydney, NSW, Australia, 1987.
33. Derbin, Y.G.; Walker, J.; Wanatowski, D.; Marshall, A.M. Numerical Simulation of Surface Subsidence after the Collapse of a Mine. In *Enhancements in Applied Geomechanics, Mining, and Excavation Simulation and Analysis*; Sevi, A., Neves, J., Zhao, H., Eds.; Springer International Publishing: Cham, Switzerland, 2019; pp. 80–97.
34. Vyazmensky, A.; Elmo, D.; Stead, D.; Rance, J. Combined Finite-Discrete Element Modelling of Surface Subsidence Associated with Block Caving Mining. In Proceedings of the 1st Canada—U.S. Rock Mechanics Symposium, Vancouver, BC, Canada, 27–31 May 2007.
35. Zhang, Z.; Mei, G.; Xu, N. A Geometrically and Locally Adaptive Remeshing Method for Finite Difference Modeling of Mining-Induced Surface Subsidence. *J. Rock Mech. Geotech. Eng.* **2022**, *14*, 219–231. [CrossRef]
36. Liu, X.; Zhang, Y.; Zhang, J.; Yang, T.; Jia, P.; Guo, R. Modelling Surface Subsidence of Coal Mines Using a Bonded Block Numerical Method. *Geomat. Nat. Hazards Risk* **2024**, *15*, 2336017. [CrossRef]
37. Li, L.; Kong, D.; Liu, Q.; Cai, H.; Chen, L. Study on Law and Prediction of Surface Movement and Deformation in Mountain Area under Repeated Mining of Shallow Coal Seam. *Bull. Eng. Geol. Environ.* **2023**, *82*, 76. [CrossRef]
38. Suchowerska Iwanec, A.M.; Carter, J.P.; Hambleton, J.P. Geomechanics of Subsidence above Single and Multi-Seam Coal Mining. *J. Rock Mech. Geotech. Eng.* **2016**, *8*, 304–313. [CrossRef]
39. Tajduś, K. New Method for Determining the Elastic Parameters of Rock Mass Layers in the Region of Underground Mining Influence. *Int. J. Rock Mech. Min. Sci.* **2009**, *46*, 1296–1305. [CrossRef]
40. Tajduś, K. Determination of Approximate Value of a GSI Index for the Disturbed Rock Mass Layers in the Area of Polish Coal Mines. *Arch. Min. Sci.* **2010**, *55*, 879–890.
41. Guo, W.; Xu, F. Numerical Simulation of Overburden and Surface Movements for Wongawilli Strip Pillar Mining. *Int. J. Min. Sci. Technol.* **2016**, *26*, 71–76. [CrossRef]
42. Jiang, Y.; Chen, B.; Teng, L.; Wang, Y.; Xiong, F. Surface Subsidence Modelling Induced by Formation of Cavities in Underground Coal Gasification. *Appl. Sci.* **2024**, *14*, 5733. [CrossRef]
43. Dudek, M.; Tajduś, K. FEM for Prediction of Surface Deformations Induced by Flooding of Steeply Inclined Mining Seams. *Geomech. Energy Environ.* **2021**, *28*, 100254. [CrossRef]
44. Zhao, J.; Konietzky, H.; Herbst, M.; Morgenstern, R. Numerical Simulation of Flooding Induced Uplift for Abandoned Coal Mines: Simulation Schemes and Parameter Sensitivity. *Int. J. Coal Sci. Technol.* **2021**, *8*, 1238–1249. [CrossRef]
45. Sakhno, I.; Sakhno, S.; Petrenko, A.; Barkova, O.; Kobylianskyi, B. Numerical Simulation of the Surface Subsidence Evolution Caused by the Flooding of the Longwall Goaf during Excavation of Thin Coal Seams. *IOP Conf. Ser. Earth Environ. Sci.* **2023**, *1254*, 012057. [CrossRef]

46. Dudek, M.; Tajduś, K.; Misa, R.; Sroka, A. Predicting of Land Surface Uplift Caused by the Flooding of Underground Coal Mines—A Case Study. *Int. J. Rock Mech. Min. Sci.* **2020**, *132*, 104377. [CrossRef]
47. Cui, F.; Li, Y.; Xu, X.; Cheng, X. Numerical Prediction of the Bridge Subsidence Induced by Longwall Mining: A Case Study of the Majiagou Bridge. *Geotech. Geol. Eng.* **2020**, *38*, 2685–2698. [CrossRef]
48. Rogowski, J.; Specht, C.; Weintrit, A.; Leszczynski, W. Evaluation of Positioning Functionality in ASG EUPOS for Hydrography and Off-Shore Navigation. *TransNav Int. J. Mar. Navig. Saf. Sea Transp.* **2015**, *9*, 221–227. [CrossRef]
49. Amadei, B. *Rock Anisotropy and the Theory of Stress Measurements*; Lecture Notes in Engineering; Springer: Berlin/Heidelberg, Germany, 1983; Volume 2, ISBN 978-3-540-12388-0.
50. Bayly, B.; Cousens, E. Deformability of Layered or Jointed Rock Masses: Analysis and Comparison of Different Types of Test. *Int. J. Rock Mech. Min. Sci. Geomech. Abstr.* **1982**, *19*, 195–199. [CrossRef]
51. Kwaśniewski, M. Mechanical Behaviour of Anisotropic Rocks. *Coprehensive Rock Eng.* **1993**, *1*, 285–312.
52. Wardle, L.J.; Gerrard, C.M. The "Equivalent" Anisotropic Properties of Layered Rock and Soil Masses. *Rock Mech. Felsmech. Méc. Roches* **1972**, *4*, 155–175. [CrossRef]
53. Tremmel, E.; Widmann, R. Das Verformungsverhalten von Gneis. In Proceedings of the 2nd ISRM Congress, Beograd, Serbia, 21–26 September 1970.
54. Nishimatsu, Y. The Torsion Test and Elastic Constant of the Orthotropic Rock Substance. In Proceedings of the 2nd ISRM Congress, Belgrade, Serbia, 21–26 September 1970.
55. Loureiro Pinto, J. Deformability of Shistous Rocks. In Proceedings of the 2nd ISRM Congress, Beograd, Serbia, 21–26 September 1970.
56. Lepper, H.A. Compression Tests on Oriented Specimens of Yule Marble. *Am. J. Sci.* **1949**, *247*, 570–574. [CrossRef]
57. AKAI, K. The Failure Surface of Isotropic and Anisotropic Rocks under Multiaxial Stresses. *J. Soc. Mater. Sci. Jpn.* **1971**, *20*, 122–128. [CrossRef]
58. Allirot, D.; Boehler, J.P. Evolutions Des Propriétés Mécaniques d'une Roche Stratifiée Sous Pression de Confinement. In Proceedings of the 4th ICISRM, Montreux, Switzerland, 8–10 October 1979; pp. 15–22.
59. Szwilski, A.B. Determination of the Anisotropic Elastic Moduli of Coal. *Int. J. Rock Mech. Min. Sci. Geomech. Abstr.* **1984**, *21*, 3–12. [CrossRef]
60. Gustkiewicz, J. Relations between the Directions of the Main Stress and Strain in a Linearly Elastic, Transversely Isotropic Medium. *Arch. Min. Sci.* **1994**, *39*, 283–300.
61. Lekhnitskii, S.G. *Theory of Elasticity of an Anisotropic Body*; Mir Publishers: Moscow, Russia, 1981.
62. Walaszczyk, J. Określenie Przemieszczeń i Naprężeń w Górotworze Niejednorodnym MES. Ph.D. Thesis, AGH University of Science and Technology in Kraków, Krakow, Poland, 1972.
63. Thin, I.G.T.; Pine, R.J.; Trueman, R. Numerical Modelling as an Aid to the Determination of the Stress Distribution in the Goaf Due to Longwall Coal Mining. *Int. J. Rock Mech. Min. Sci. Geomech. Abstr.* **1993**, *30*, 1403–1409. [CrossRef]
64. Mielimąka, R.; Wesołowski, M. Modelowanie Metodą Elementów Skończonych Wieloetapowego Procesu Obniżeń i Odkształceń Poziomych Terenu Górniczego. *Zesz. Nauk. Politech. Śląskiej Seria Górnictwo* **2004**, *70*, 251–261.
65. Marinos, P.; Hoek, E. GSI: A Geologically Friendly Tool for Rock Mass Strength Estimation. In Proceedings of the GeoEng2000 Conference, Melbourne, Australia, 19–24 November 2000; pp. 1422–1442.
66. Hoek, E. Strength of Rock & Rock Masses. *ISRM News J.* **1994**, *2*, 4–16.
67. Hoek, E.; Brown, E.T. Practical Estimates of Rock Mass Strength. *Int. J. Rock Mech. Min. Sci.* **1997**, *34*, 1165–1186. [CrossRef]
68. Nelder, J.A.; Mead, R. A Simplex Method for Function Minimization. *Comput. J.* **1965**, *7*, 308–313. [CrossRef]
69. Spendley, W.; Hext, G.R.; Himsworth, F.R. Sequential Application of Simplex Designs in Optimisation and Evolutionary Operation. *Technometrics* **1962**, *4*, 441–461. [CrossRef]
70. Polanin, P. Application of Two Parameter Groups of the Knothe–Budryk Theory in Subsidence Prediction. *J. Sustain. Min.* **2015**, *14*, 67–75. [CrossRef]
71. Stoch, T. Wpływ Warunków Geologiczno-Górniczych Eksploatacji Złóż Na Losowość Procesu Przemieszczeń i Deformacji Powierzchni Terenu. Ph.D Thesis, AGH University of Science and Technology in Kraków, Krakow, Poland, 2005.
72. Tajduś, K. *Determination of the Value of the Strain Parameters for Strata Rock Mass in the Region of Underground Mining Influence*; Issue 2; VGE Verlag GmbH: Essen, Germany, 2009.
73. Narimani, S.; Davarpanah, S.M.; Kovács, L.; Vásárhelyi, B. Variation of Elastic Stiffness Parameters of Granitic Rock during Loading in Uniaxial Compressive Test. *Appl. Mech.* **2023**, *4*, 445–459. [CrossRef]
74. Dubiński, J.; Mutke, G.; Chodacki, J. Distribution of Peak Ground Vibration Caused by Mining Induced Seismic Events in the Upper Silesian Coal Basin in Poland. *Arch. Min. Sci.* **2020**, *65*, 419–432. [CrossRef]
75. Mills, K.W.; O'Grady, P. Impact of Longwall Width on Oberburden Behaviour. In *Proceedings of the Coal 1998: Coal Operators' Conference*; Aziz, N., Ed.; University of Wollongong and the Australian Institute of Mining and Metallurgy: Wollongong, Australia, 1998; pp. 147–155.
76. Mills, K.; Waddington, A.A.; Holla, L. *Subsidence Engineering*; Australian Institute of Mining and Metallurgy: Melbourne, VIC, Australia, 2009; pp. 874–902.
77. McNally, G.H.; Willey, P.L.; Creech, M. Geological Factors Influencing Longwall-Induced Subsidence. In Proceedings of the Proceedings Symposium on Geology in Longwall Mining, Sydney, NSW, Australia, 28–30 October 1996; pp. 257–267.

78. Borecki, M.; Knothe, S. *Ochrona Powierzchni Przed Szkodami Górniczymi*; Wydawnictwo Śląsk: Katowice, Poland, 1980.
79. Wesołowski, M. *Zastosowanie Liniowego Ośrodka Transwersalnie Izotropowego do Modelowania Deformacji Terenu Górniczego*; Wydawnictwo Politechniki Śląskiej: Gliwice, Poland, 2013.